Andean Geology 53 (2): 225-241 May, 2026
doi: 10.5027/andgeoV53n2-3845

Andean Geology
www.andeangeology.cl

SPECIAL ISSUE: RESEARCH ON THE SOUTH WEST MARGIN OF GONDWANA

South Georgia in a West Gondwana context: detrital zircon geochronology of a late Permian accretionary complex

***Teal R. Riley[1], Andrew Carter[2], Michael J. Flowerdew[3], Ian L. Millar[4], Martin J. Whitehouse[5]**

[1] *British Antarctic Survey, High Cross, Madingley Road, Cambridge, CB3 0ET, UK.*
trr@bas.ac.uk
[2] *Department of Earth and Planetary Sciences, Birkbeck, University of London, Malet Street, London WC1E 7HX, UK.*
a.carter@ucl.ac.uk
[3] *CASP, Madingley Rise, Madingley Road, Cambridge CB3 0UD, UK.*
michael.flowerdew@casp.org.uk
[4] *British Geological Survey, Keyworth, Nottingham, NG12 5GG, UK.*
ilm@bgs.ac.uk
[5] *Swedish Museum of Natural History, Frescativägen 40, 114 18 Stockholm, Sweden.*
martin.whitehouse@nrm.se

**Author for correspondence: trr@bas.ac.uk*

ABSTRACT. South Georgia lies in a remote position in the circumpolar South Atlantic and is one of the most isolated continental fragments on Earth. The basement geology of South Georgia is restricted to the southeast sector of the island and is termed the Drygalski Fjord Complex, which consists of metasedimentary rocks and localised paragneisses that form an accretionary complex cut by multiple dolerite dykes and gabbroic intrusive rocks. We examine the detrital zircon geochronology and geochemistry of six metasedimentary samples from the Drygalski Fjord Complex to determine their depositional and provenance history and explore correlations to elsewhere in West Gondwana. The basal Salomon Glacier Formation has a maximum depositional age of *ca*. 270 Ma and a secondary age peak at *ca*. 470 Ma that is consistent with West Gondwana accretionary complexes from the northern Antarctic Peninsula and Patagonia. This depositional age is also shared with sedimentary successions from the Karoo Basin (South Africa) and East Antarctica, but they lack the secondary age peak (*ca*. 470 Ma), being instead characterised by an age peak at *ca*. 530 Ma, associated with the recycled Cambrian sources of East Antarctica. The late Permian accretionary complex of South Georgia is closely correlated to units from the northern Antarctic Peninsula (Trinity Peninsula Group) and the southern Cordillera Darwin, and we favour a common origin on the Antarctic Plate before closure of the Rocas Verdes Basin and translation to the Scotia Plate.

Keywords: Antarctic, Provenance, Patagonia, Lu-Hf isotopes.

RESUMEN. Georgia del Sur en el contexto de Gondwana Occidental: geocronología de circones detríticos de un complejo acrecionario del Pérmico tardío. Georgia del Sur se encuentra en una posición remota del Atlántico Sur circumpolar y constituye uno de los fragmentos continentales más aislados del planeta. La geología del basamento de la isla está restringida al sector suroriental y se conoce como el Complejo Drygalski Fjord, compuesto por rocas metasedimentarias y paragneises localizados que conforman un complejo acrecionario intruido por numerosos diques de dolerita y cuerpos gabroicos. En este estudio analizamos la geocronología y geoquímica de circones detríticos de seis muestras metasedimentarias del Complejo Drygalski Fjord, con el fin de determinar su historia de depositación y proveniencia, así como explorar sus posibles correlaciones con otras regiones de Gondwana Occidental. En la base de este complejo, la Formación Salomon Glacier tiene una edad máxima de depositación de *ca*. 270 Ma y una población secundaria de circones detríticos de *ca*. 470 Ma, lo cual es consistente con los complejos acrecionarios de Gondwana Occidental ubicados en el norte de la Península Antártica y Patagonia. Edades de depositación similares se han observado

en sucesiones sedimentarias de la Cuenca del Karoo (Sudáfrica) y en la Antártica Oriental; sin embargo, estas últimas carecen de la población de circones de *ca.* 470 Ma, y presentan, en cambio, otra de *ca.* 530 Ma, asociada a fuentes recicladas del Cámbrico de la Antártica Oriental. El complejo acrecionario del Pérmico tardío de Georgia del Sur muestra una estrecha correlación con unidades del norte de la Península Antártica (Grupo de la Península Trinidad) y del sur de la cordillera Darwin, por lo que consideramos más probable un origen común en la placa Antártica, previo al cierre de la Cuenca Rocas Verdes y a su posterior traslación hacia la placa Scotia.

Palabras clave: Antártica, Proveniencia, Patagonia, Isótopos Lu-H.

1. Introduction

South Georgia is a remote island in the South Atlantic Ocean, lying approximately 1,700 km east of the southern tip of South America. The island is situated towards the eastern extremity of the North Scotia Ridge (Fig. 1), which defines a transform plate boundary between the South American and Scotia plates (Livermore *et al.*, 1994). The North Scotia Ridge is a long-lived strike-slip system that accommodated oceanic spreading during the opening of the Scotia Sea and consists of several, mostly submerged, continental crustal blocks in a linear chain from Tierra del Fuego to South Georgia. The broad consensus (*e.g.* Carter *et al.*, 2014; Dalziel *et al.*, 2021; Beaver *et al.*, 2022) is that from at least the Cretaceous until the Eocene, the South Georgia microcontinent was a continuation of the Andean Cordillera until Eocene separation and translation to its current location. Dalziel *et al.* (2021) highlighted the similarities in sedimentary successions between Tierra del Fuego and South Georgia, and proposed that South Georgia originated in the Staten Embayment (Fig. 1). These correlations are supported by detrital zircon provenance analysis of sedimentary successions from South Georgia, Fuegian Andes and the North Scotia Ridge (Barbeau *et al.*, 2010; Carter *et al.*, 2014; Riley *et al.*, 2019).

However, a fundamental problem with a contiguous relationship between Tierra del Fuego and South Georgia during the Late Cretaceous is that analysis of seafloor spreading along the West Scotia Ridge can only accommodate approximately half of the strike-slip translation along the North Scotia Ridge required for the post-Eocene separation between Tierra del Fuego and South Georgia (Eagles, 2010). Dalziel *et al.* (2021) also acknowledged that the Scotia Sea tectonic history could not fully explain the present-day location of South Georgia and suggested that 'escape tectonics' during the Late

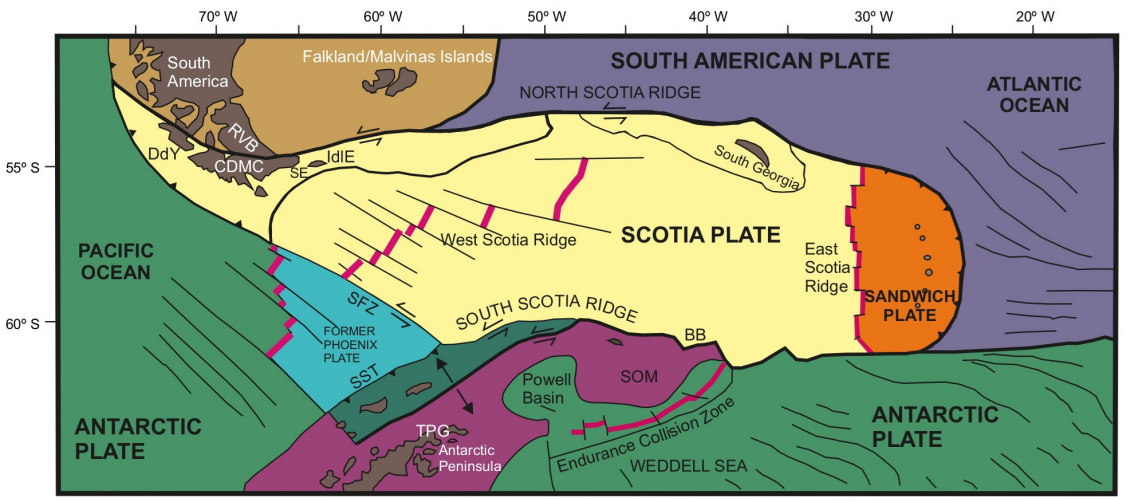

FIG. 1. Tectonic setting of the Scotia Sea (adapted from Riley *et al.*, 2022). **BB**: Bruce Bank; **CDMC**: Cordillera Darwin metamorphic complex; **DdY**: Duque de York Complex; **IdlE**: Isla de los Estados (Staten Island); **RVB**: Rocas Verdes Basin; **SE**: Staten Embayment; **SFZ**: Shackleton Fracture Zone; **SOM**: South Orkney microcontinent; **SST**: South Shetland trough; **TPG**: Trinity Peninsula Group.

Cretaceous along transcurrent faults may have also played a role.

One aspect that has not been fully addressed is the paleo-location of South Georgia during the late Palaeozoic-early Mesozoic, prior to the breakup of Gondwana. Eagles (2010) and Eagles and Eisermann (2020) proposed that South Georgia originated within the interior of Gondwana, where it must have had a paleo-location to the east of a 'barrier' of thick oceanic lithosphere between the Falkland Plateau and central Scotia Sea basins. They argued that the main stratigraphic elements of South Georgia's Mesozoic and late Palaeozoic history are ubiquitous throughout West Gondwana and are not uniquely diagnostic. Eagles and Eisermann (2020) suggested that detrital zircon age profiles from mid- to Late Cretaceous sedimentary successions on South Georgia could have been derived from magmatic and recycled sources in South Africa as opposed to the Andean Cordillera.

In this work we examine, for the first time, the basement metasedimentary succession of South Georgia to explore potential correlations with South America, Antarctic Peninsula, East Antarctica and South Africa in the late Permian, and to provide a test for a South Georgia-South Africa connection. Six metasedimentary siliciclastic samples from the basement Salomon Glacier Formation and Cooper Island Formation of the Drygalski Fjord Complex were analysed for their detrital zircon U-Pb age population, combined with a subset of Lu-Hf isotope analysis, and calculations of maximum depositional age.

2. Geological setting

The basement geology of South Georgia is restricted to the southeast sector of the island (Fig. 2) and is composed of two distinct complexes, probably separated by a fault (Macdonald *et al.*, 1987). The Drygalski Fjord Complex was defined by Storey (1983) and is characterised by a suite of highly deformed metasedimentary rocks and paragneisses intruded by multiple mafic plutons, leading to localised hornfels texture. Storey (1983) also highlighted the presence of local migmatite layers associated with paragneisses. The Drygalski Fjord Complex has three spatially distinct metasedimentary successions that can be identified in the Salvesen Range, adjacent to Drygalski Fjord and Cooper Island (Fig. 2): the Salomon Glacier, Novosilski Glacier and Cooper Island formations (Dalziel *et al.*, 2021). The age of deposition of the metasedimentary rocks of the Drygalski Fjord Complex is uncertain, but it is intruded by Early Jurassic plutons (Tanner and Rex, 1979; Curtis *et al.*, 2010), some of which are anatectic (Tanner and Rex, 1979). The basal Salomon Glacier Formation, which is the focus of this study, has been subject to higher grade metamorphism (?Buchan-type) and greater deformation than the Cooper Island and Novosilski formations, and as such may not represent a direct equivalent.

To the west of the Drygalski Fjord Complex is the Larsen Harbour Complex (Fig. 2), which is interpreted as an ophiolite sequence consisting of a succession, up to 2 km in thickness, of tholeiitic pillow basalts, massive lavas and intercalated chert, cut by multiple mafic dykes (Mair, 1987). It has also been correlated with the Tortuga and Sarmiento ophiolite complexes of South America (Dalziel *et al.*, 2021). The Larsen Harbour and Drygalski Fjord complexes were together interpreted as a Gondwana margin accretionary complex that was subject to crustal thinning during the Late Jurassic (Mukasa and Dalziel, 1996).

The major part of South Georgia is dominated by Lower Cretaceous (Carter *et al.*, 2014) turbidite sequences that were deposited in a back-arc basin setting and are separated from the basement units by the Cooper Bay shear zone (Curtis *et al.*, 2010) (Fig. 2). Two laterally equivalent units are identified, the extensive Cumberland Bay Formation and the more spatially restricted Sandebugten Formation (Fig. 2). The Cumberland Bay Formation is up to 8 km in thickness and consists of volcaniclastic greywackes of andesitic composition deposited in a continental margin magmatic arc setting that was deformed into large-scale (>100 m) folds associated with low-grade regional metamorphism. The Cumberland Bay Formation is host to a probable Lower Cretaceous (Aptian) fossil (ichnofauna) assemblage (Macdonald, 1982). The adjacent Sandebugten Formation is a more siliciclastic quartz-rich sandstone and shale turbidite sequence, inferred by Dalziel *et al.* (1975) to be derived from the continental margin.

Volcanic arc rocks are restricted to Annenkov Island and Pickersgill Islands (Fig. 2) to the west of South Georgia. The units exposed are distinct to the lithologies of the main island. The Annenkov Island Formation is formed of andesitic tuffs and breccias that have a total thickness of almost 2 km (Pettigrew, 1981) and are probably Cretaceous in age (Dalziel *et al.*, 2021).

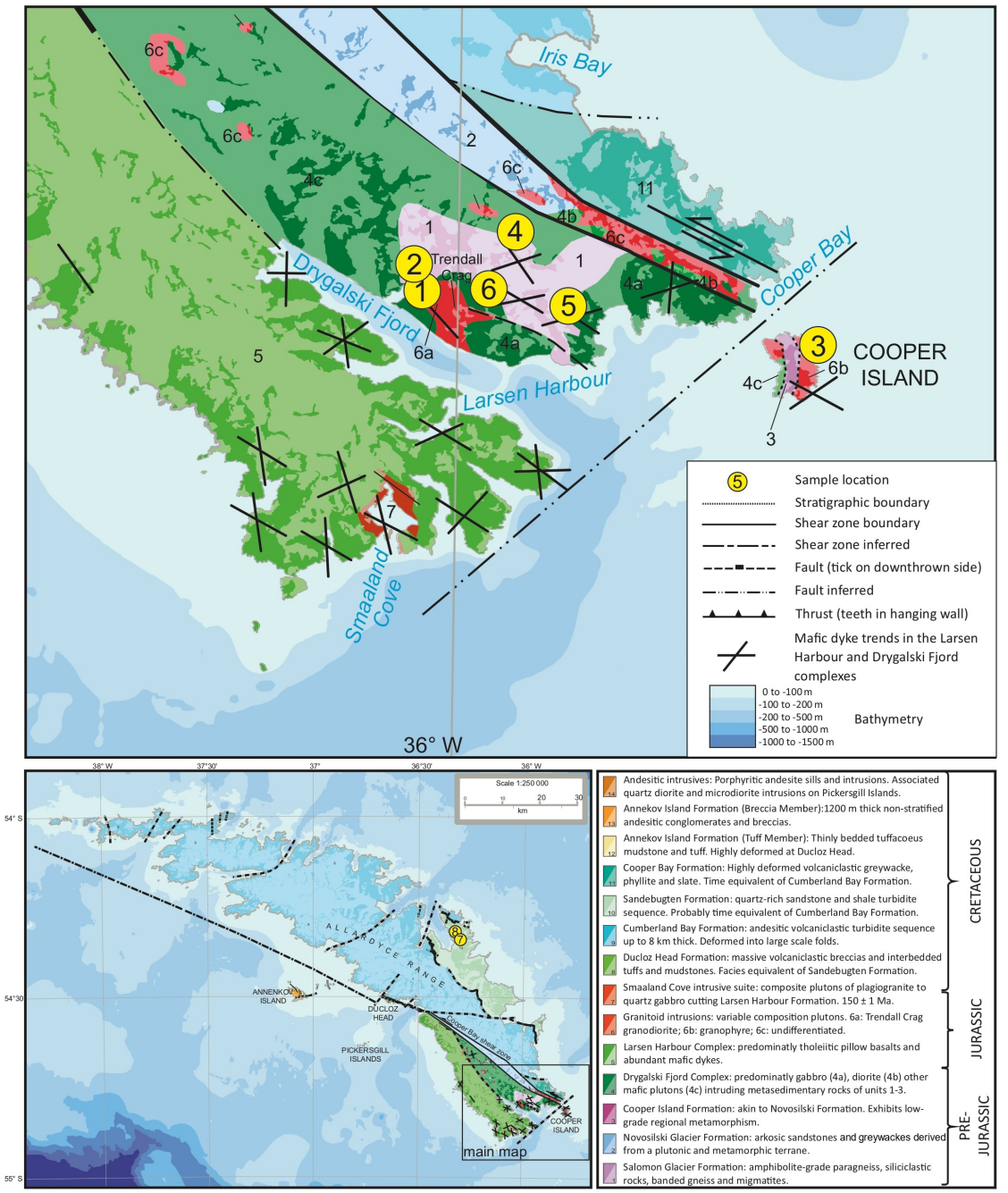

FIG. 2. Geological map of South Georgia, modified from Curtis (2011). Darker areas show the extent of rock outcrop, with the paler areas showing inferred geology. Sample locations (see Table 1 for precise positional information): **1**. M.2022.1a; **2**. M.2025.3; **3**. M.4131.15; **4**. M.2171.8b; **5**. M.1683CMB2.12; **6**. M.2042.1d; **7**. SG7.389.1 (54.33670° S, 36.32457° W); **8**. SG7.394.1 (54.33611° S, 36.34062° W).

A potential facies equivalent of the Annenkov Island volcanic rocks is the Ducloz Head Formation (Fig. 2) consisting of massive volcaniclastic breccias and interbedded tuffs, although Storey (1983) also raised the possibility that components of it may be related to the Sandebugten Formation. Another potentially related metasedimentary succession identified as the Cooper Bay Formation is restricted to the southeast corner of the island and is a likely facies variation of the Cumberland Bay Formation (Clayton, 1982).

Magmatic rocks have a limited areal extent across South Georgia, with the main concentration cropping out in the southeast of the island along the Cooper Bay shear zone, Larsen Harbour, Smaaland Cove and outlying islands (Fig. 2). Several of the granitoid plutons have been dated (Mukasa and Dalziel, 1996; Curtis *et al.*, 2010) and have yielded Middle-Late Jurassic (*ca.* 160-150 Ma) U-Pb zircon ages from the Cooper Bay shear zone, Larsen Harbour Complex and Smaaland Cove intrusive suite. Earlier geochronology on granitoid rocks by Tanner and Rex (1979) yielded Rb-Sr and K-Ar ages from the Early Jurassic to mid-Cretaceous, but with concerns over reliability.

3. Sample selection

Six samples (British Antarctic Survey archive collection) from the Drygalski Fjord Complex of South Georgia were selected for detrital zircon provenance analysis; four from the basement Salomon Glacier Formation (M.2022.1a, M.1683CMB2.12, M.2025.3, M.2042.1d), one from the Cooper Island Formation (M.4131.15), and one undifferentiated sample (M.2171.8b). All samples are medium- to coarse-grained siliciclastic metasedimentary rocks. Their location is shown in figure 2 and positional information is provided in table 1.

4. Analytical methods

4.1. U-Pb zircon geochronology

Zircon (U-Pb) geochronology was carried out at University College London and the Swedish Museum of Natural History. Full analytical procedures, data (Supplementary Table S1) and representative spot location images (Supplementary Fig. S1) are provided in the Supplementary Material. A summary of the analytical procedures is detailed here.

Heavy minerals were separated from bulk sieved (<300 µm) crushed rock using standard density liquid and magnetic separation procedures. Zircon-enriched extracts were mounted in hard epoxy resin on glass slides and polished for analysis. Zircon crystals were typically in the size range 100-180 µm, with a range of grain sizes analysed for all samples. Zircon U-Pb geochronology on four of the samples (M.2022.1a, M.2025.3, M.4131.15, M.2171.8b) was carried out at University College London (November 2023) using laser ablation inductively coupled mass spectrometry (LA-ICP-MS) facilities (Agilent 7700 coupled to a New Wave Research 193 nm excimer laser) at the London Geochronology Centre. Typical laser spot sizes of 25 µm were used with a 7-10 Hz repetition rate and a fluence of 2.5 J/cm^2, and the outer parts of the grain were analysed. Background measurement before ablation lasted 15 seconds and laser ablation dwell time was 25 seconds. The external zircon standard was Plešovice, which has a TIMS reference age of 337.13±0.37 Ma (Sláma *et al.*, 2008). Standard errors on isotope ratios and ages included the standard deviation of $^{206}Pb/^{238}U$ ages of the Plešovice standard zircon. Time-resolved signals that record isotopic ratios with depth in each crystal were processed using GLITTER 4.5, developed by the ARC National Key Centre for Geochemical Evolution and Metallogeny of Continents (GEMOC) at Macquarie University and CSIRO Exploration and Mining, Australia. Processing enabled filtering to remove spurious signals owing to overgrowth boundaries, weathering, inclusions, or fractures. Ages were calculated using the $^{206}Pb/^{238}U$ ratios for samples dated as <1.1 Ga, and the $^{207}Pb/^{206}Pb$ ratios for older grains. Discordance was determined using ($^{207}Pb/^{235}U$-$^{206}Pb/^{238}U$)/($^{206}Pb/^{238}U$) and similar for $^{207}Pb/^{206}Pb$ ages.

At the Swedish Museum of Natural History (Stockholm), U-Pb ion-microprobe zircon geochronology was carried out using a CAMECA 1280 ion microprobe at the NordSIMS facility (March 2024) on two further samples (M.1683CMB2.12, M.2042.1d). The analytical method closely followed Whitehouse and Kamber (2005) but differed insomuch that the oxygen ion primary beam was generated using a high-brightness, radiofrequency plasma ion source (Oregon Physics, Hyperion II) rather than a duoplasmatron, and a focused beam instead of illuminated aperture. The 10 nA O_2- beam was rastered over 5x5 µm to homogenize beam

TABLE 1. SAMPLE LOCATION AND DETRITAL ZIRCON AGE INFORMATION.

Sample ID	N° in figure 2	Lithology	Placename	Latitude	Longitude	Formation	Detrital zircon age peaks (Ma)	Maximum likely depositional age (Ma)
M.2022.1a	1	Meta-sandstone	Drygalski Fjord	-54.78651	-36.02287	Salomon Glacier Formation	265, 469	255±6
M.2025.3	2	Banded paragneiss	Drygalski Fjord	-54.77816	-36.02333	Salomon Glacier Formation	266, 469	265±3
M.4131.15	3	Quartz-rich meta-sandstone	Cooper Island	-54.80569	-35.77369	Cooper Island Formation	283, 474	271±3
M.2171.8b	4	Meta-sandstone	Salomon Glacier	-54.75470	-35.90452	Drygalski Fjord Complex	253, 431	195±6
M.1683CMB2.12	5	Meta-sandstone	Hamilton Bay	-54.80946	-35.91921	Salomon Glacier Formation	272, 472	274±4
M.2042.1d	6	Paragneiss	Drygalski Fjord	-54.78991	-35.96936	Salomon Glacier Formation	267, 477	270±3

density, the final analytical spot size being ~15 µm in diameter. Sputtered secondary ions introduced into the mass spectrometer were analysed using a single ion counting electron multiplier over 10 cycles of data. Data were reduced using in-house developed software. The power law relationship between $^{206}Pb/^{238}U^{16}O$ and $^{238}U^{16}O_2/^{238}U^{16}O$ measured from the 91500 standard was used to calibrate U/Pb ratios following the recommendations of Jeon and Whitehouse (2015). Common-Pb corrections were applied to analyses where statistically significant ^{204}Pb was detected, using the present-day terrestrial common-Pb estimate of Stacey and Kramers (1975). ^{207}Pb corrected ages were calculated assuming non-radiogenic Pb was from surface contamination and had an isotopic composition of modern-day average terrestrial common-Pb ($^{207}Pb/^{206}Pb$=0.836; Stacey and Kramers, 1975).

4.2. Lu-Hf isotope analysis

Lu-Hf isotopes were determined on just one of the samples from the Salomon Glacier Formation (M.2042.1d), using the same spot location as for the U-Pb dating. The analyses were determined (April 2024) on a Neptune multi-collector inductively coupled plasma-mass spectrometer (MC-ICP-MS) coupled with a laser ablation system at the British Geological Survey. Initial $^{176}Hf/^{177}Hf$ ratios were calculated using the U-Pb crystallisation age of each grain and the results are expressed as initial εHf (εHf_i). εHf values were calculated using a ^{176}Lu decay constant of $1.867x10^{-11}$ y^{-1} (Söderlund *et al.*, 2004), a present-day chondritic $^{176}Lu/^{177}Hf$ value of 0.0336, and a $^{176}Hf/^{177}Hf$ ratio of 0.282785 (Bouvier *et al.*, 2008). Full analytical details are provided in the Supplementary Material and results are presented in the Supplementary Table S2.

5. Results

5.1. U-Pb detrital zircon geochronology

The age distributions of the six analysed samples are displayed as kernel density estimator plots (KDE) in figure 3. They are plotted alongside the age distributions from two samples from the Cretaceous Sandebugten Formation (Carter *et al.*, 2014) to illustrate their Permian age contributions. The analysed samples have very few ages >1,200 Ma (Supplementary Table S1), and these are omitted from the KDE plots to better illustrate the Palaeozoic age profiles. The six samples from the broader Drygalski Fjord Complex all have similar age profiles characterised by prominent late Permian and Early Ordovician age peaks, and a minor Devonian age peak (Fig. 3; Table 1). Each sample is also characterised by a broad range of Neo-and Mesoproterozoic age zircons. However, there are also notable distinctions in the age profiles, with the four samples from the Salomon Glacier Formation characterised by clear age peaks at *ca*. 270 and *ca.* 470 Ma (Fig. 3; Table 1), whilst the sample from the Cooper Island Formation has an older Permian age peak (*ca.* 283 Ma), and the sample from the undifferentiated Drygalski Fjord Complex (M.2171.8b) has a younger Permian age peak (*ca.* 253 Ma) and no clearly defined Early Ordovician age peak. The two samples from the Sandebugten Formation, although dominated by mid-Cretaceous and Middle Jurassic age peaks also have significant late Permian and minor Early Ordovician age peaks. The late Permian age peaks from the Cretaceous units are distinct, with one sample having a peak at *ca*. 250 Ma and the other at *ca*. 270 Ma.

5.2. Maximum depositional age

In the absence of diagnostic fossil assemblage and no dateable volcanic beds, detrital zircon geochronology is a valuable technique to provide an estimate on the depositional age of siliciclastic rocks. We follow the approach of Vermeesch (2021), who applied the maximum likelihood algorithm of Galbraith and Laslett (1993) to determine the maximum depositional age (MDA). The results for the six samples from the Drygalski Fjord Complex are presented as radial plots (Supplementary Fig. S2) where the minima are used to derive the MDA (Table 1).

The samples from the Drygalski Fjord Complex and its component formations are dominated by middle to late Permian MDAs, typically in the range, 265-275 Ma (Table 1; Supplementary Fig. S2). One sample (M.2022.1a) has a younger MDA of 255±6 Ma and is consistent with a marginally younger primary age peak. Sample M.2171.8b, from the undifferentiated Drygalski Fjord Complex yields a significantly younger MDA (195±6 Ma) with a primary age peak of *ca.* 253 Ma. This sample is characterised by a significant (n=23) number of Early Jurassic-Triassic

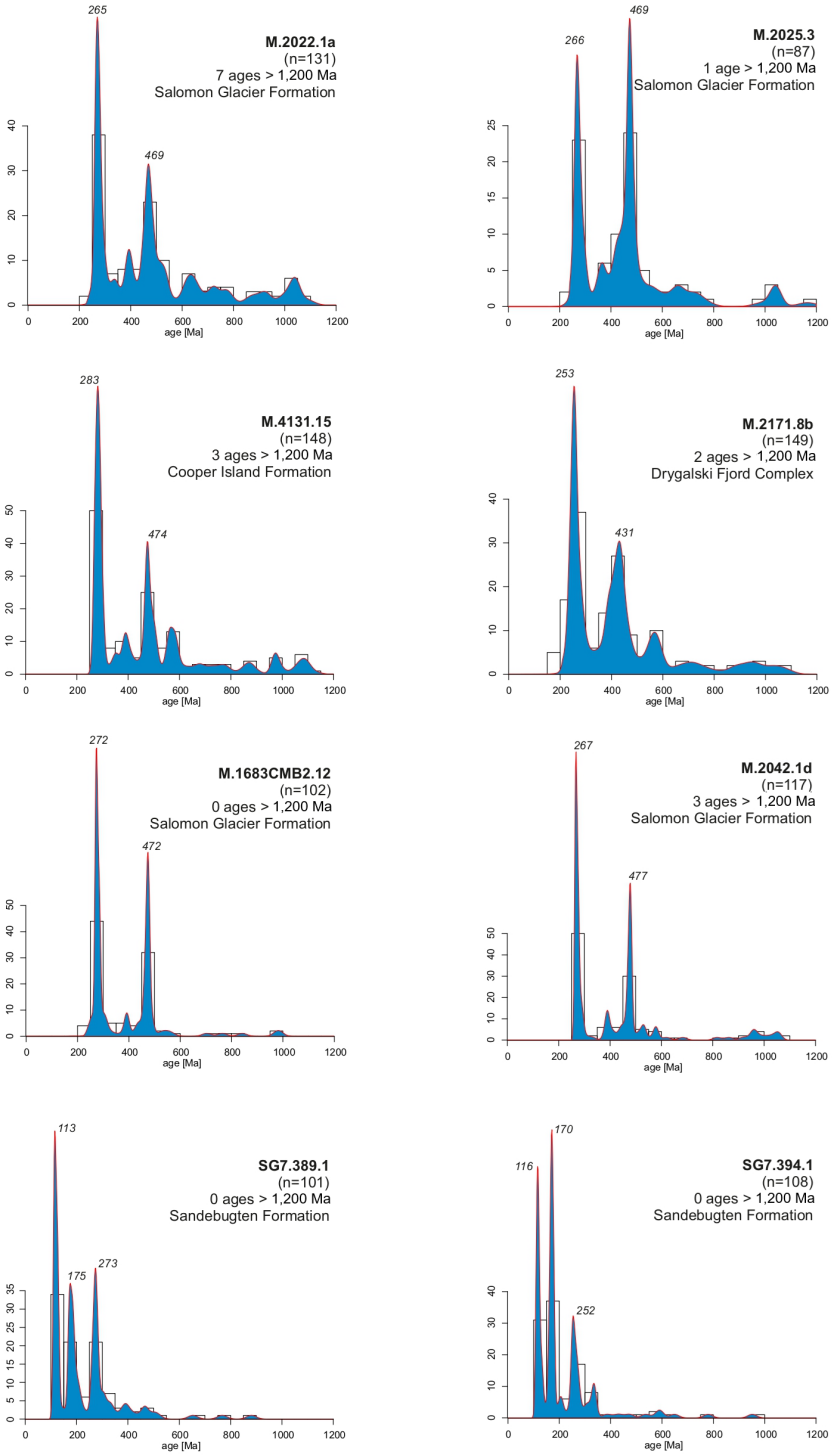

FIG. 3. Kernel density estimator (KDE) plots (Vermeesch, 2013) of U-Pb detrital zircon ages for metasedimentary rocks from the Drygalski Fjord Complex (this study) and from the Sandebugten Formation (Carter *et al.*, 2014). Full datasets are available in Supplementary Table S1. Analytical details in Supplementary Material. Bandwidths for all plotted samples are 50 Myr. The area under the KDE plots in not normalised and an adaptive kernel bandwidth was applied. Sample locations as shown in figure 2.

zircon grains and may represent an episode of early Mesozoic accretion and recycling that developed in West Gondwana accretionary provinces (Trouw *et al.*, 1997; Flowerdew *et al.*, 2007; Riley *et al.*, 2023a).

5.3. Multi-dimensional scaling analysis

Multi-dimensional scaling analysis (MDS) is a valuable tool to help determine which sedimentary units may correlate in terms of their age profile and common source regions. The samples from the Drygalski Fjord Complex (excluding M.2171.8b; see section 5.1) are plotted in figure 4 in comparison to a range of middle to late Permian sedimentary successions from South America, Antarctic Peninsula, East Antarctica, South Africa and the Falkland/Malvinas Islands (full comparative data sources in Supplementary Table S3). All samples have broadly similar age profiles dominated by a primary late Permian age peak at *ca*. 270 Ma (Fig. 5). However, the secondary age peak at *ca*. 470 Ma evident from the South Georgia basement unit is only pronounced for the Trinity Peninsula Group (Antarctic Peninsula), the southern Cordillera Darwin and the Duque de York Complex (Patagonia). The MDS plot highlights this observation, with the late Permian Salomon Glacier Formation having a close relationship to the middle Trinity Peninsula Group, the southern Cordillera

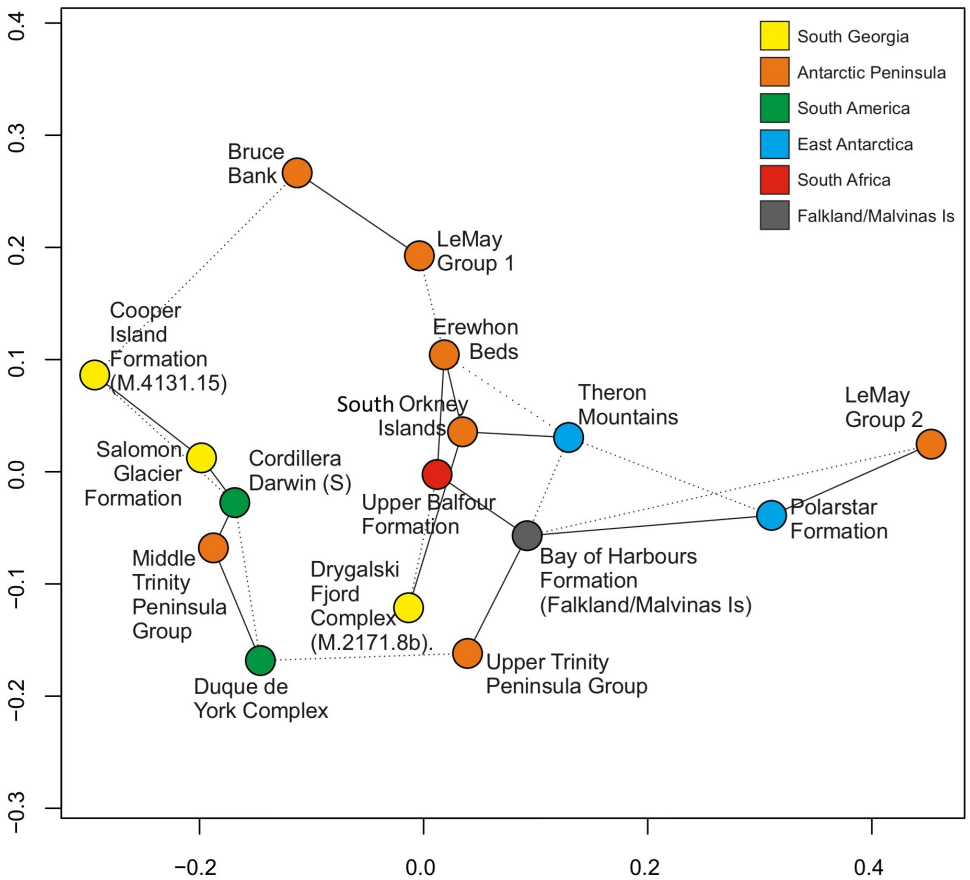

FIG. 4. Multidimensional scaling maps (MDS; Vermeesch, 2013, 2018) for late Permian sedimentary units from West Gondwana. MDS plots compare the complete age spectra in dissimilar samples calculated using the Kolmogorov-Smirnov statistic with any two points plotting closer together if they are more similar. Nearest (solid) and secondary (dashed) neighbour lines are shown. The axis scales are dimensionless and have no physical meaning. Data from Hervé *et al.* (2003, 2010), Barbeau *et al.* (2010), Flowerdew *et al.* (2012), Elliot *et al.* (2016), Castillo *et al.* (2016), Carter *et al.* (2017), Craddock *et al.* (2017), Viglietti *et al.* (2018), Nelson and Cottle (2019), and Riley *et al.* (2022, 2023a,b, 2025). A detailed list of late Permian data sources is provided in Supplementary Table S3. Salomon Glacier Formation (M.2022.1a, M.2025.3, M.2042.1d, M.1683CMB2.12); Cooper Island Formation (M.4131.15); Drygalski Fjord Complex (M.2171.8b).

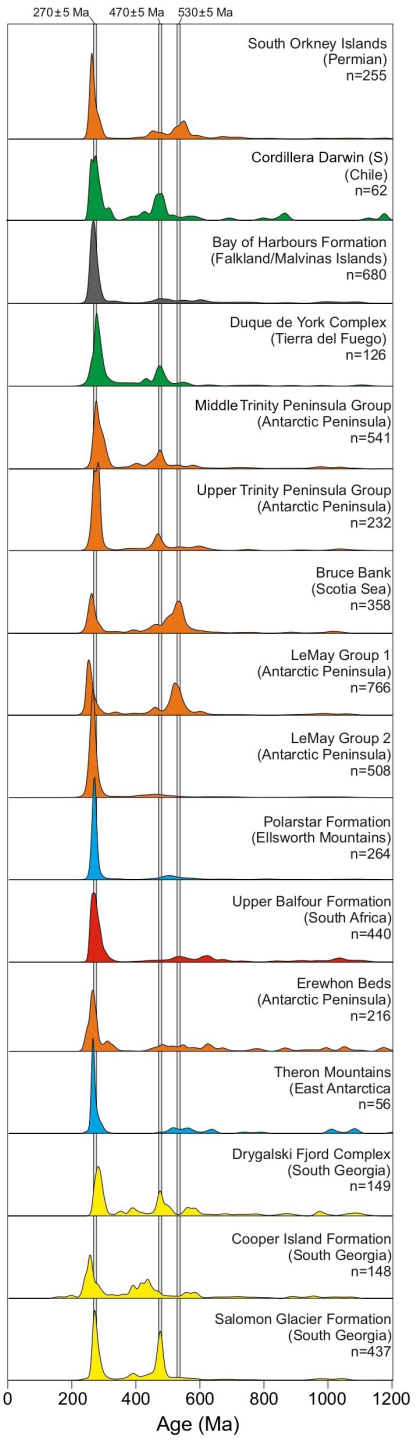

FIG. 5. U-Pb age stacked (KDE) plots for mid-late Permian samples. Grey bars represent significant zircon peaks at *ca.* 270±5 Ma, *ca.* 470±5 Ma and *ca.* 530±5 Ma. Data sources as in figure 4. The area under the KDE plots is normalised and an adaptive kernel bandwidth was applied. Data sources are provided in Supplementary Table S3.

Darwin and, to a lesser degree, the Duque de York Complex. Late Permian sedimentary units from South Africa have a close relationship to sedimentary rocks from the Falkland/Malvinas Islands, Theron Mountains (East Antarctica), Polarstar Formation (Ellsworth Mountains) and the Erewhon Beds of the southern Antarctic Peninsula (Fig. 6A) as highlighted by Riley *et al.* (2025). Late Permian accretionary complexes from the LeMay Group of the southern Antarctic Peninsula and the Bruce Bank of the southern Scotia Sea (Fig. 6A) have a more distant relationship to the metasedimentary units from South Georgia and generally lack an age population at *ca*. 470 Ma but a more prominent Cambrian peak at *ca*. 530 Ma that is absent from the metasedimentary units of South Georgia.

Overall, there is a significant overlap across all late Permian sedimentary successions from West Gondwana, but the units from South Georgia, particularly the Salomon Glacier Formation, share the closest relationship to the accretionary complexes from the northern Antarctic Peninsula (Trinity Peninsula Group) and metasedimentary rocks of southern Patagonia (Cordillera Darwin and Duque de York Complex).

5.4 Lu-Hf isotopes

Age-adjusted Lu-Hf isotope data complement zircon U-Pb age data to provide improved controls on provenance and correlation of sedimentary units, with a common source (*e.g.*, Riley *et al.*, 2023b). Lu-Hf isotopic analysis was undertaken on a single sample (M.2042.1d) from the Drygalski Fjord Complex (Salomon Glacier Formation) that was also analysed for U-Pb geochronology. The data are plotted in figure 7A alongside data from late Permian sedimentary successions from Patagonia and the northern Antarctic Peninsula. The analysed sample from the Salomon Glacier Formation has late Permian εHf_i values in the range -5 to +2. There is a broad overlap in εHf_i values for the late Permian age population between the metasedimentary units from South Georgia, Trinity Peninsula Group and Duque de York Complex. The sample from the Salomon Glacier Formation analysed for Lu-Hf isotopes exhibits a closer relationship to the late Permian Trinity Peninsula Group than to the Duque de York Complex, with an overlap in more juvenile values (>0), which are absent in the Duque de York Complex. This close relationship is also evident in the MDS plot (Fig. 4).

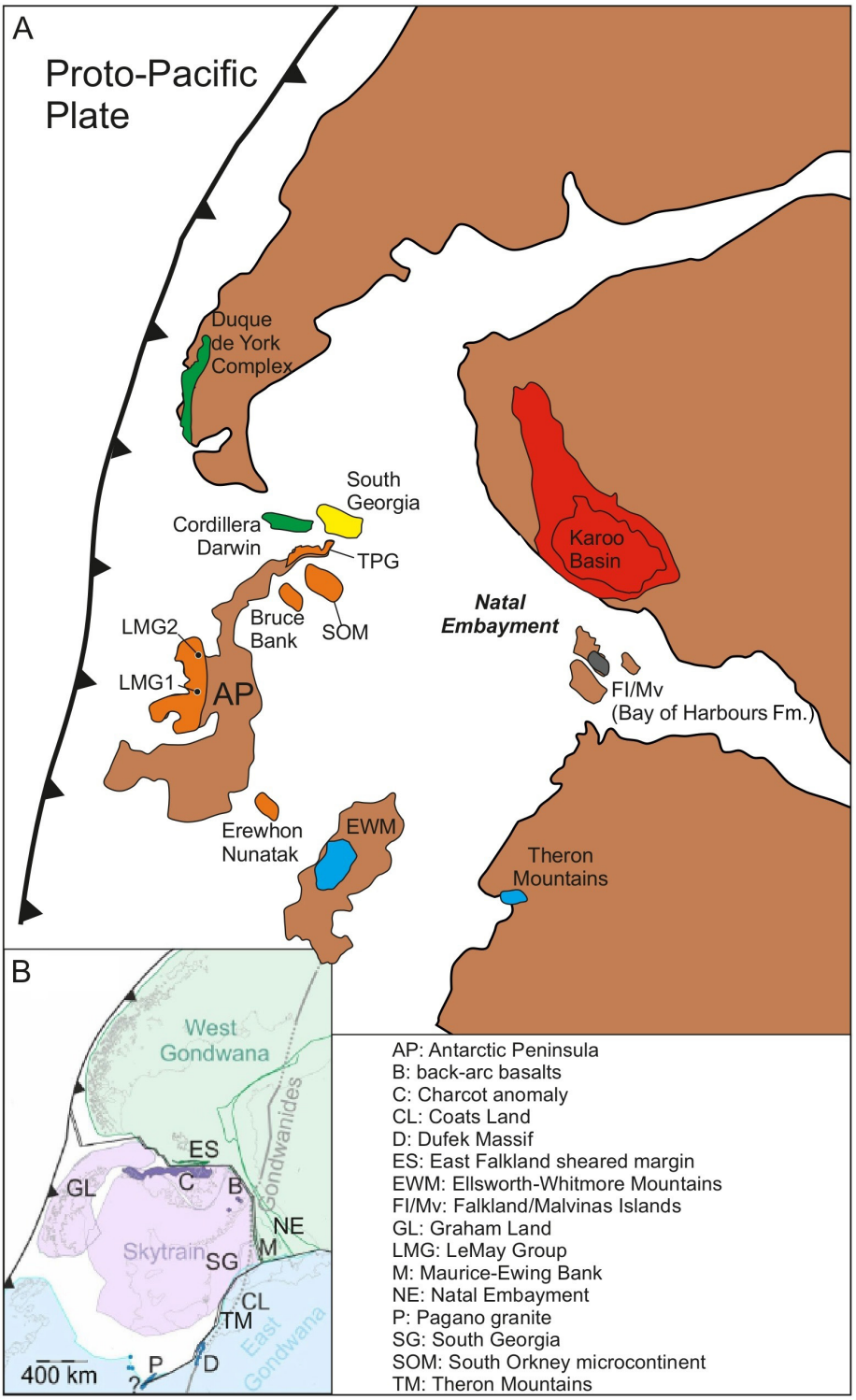

FIG. 6. **A.** Late Permian reconstruction of West Gondwana, adapted from Riley *et al.* (2025). **B.** Early Mesozoic plate reconstruction from Eagles and Eisermann (2020) showing the putative Skytrain Plate (purple domain).

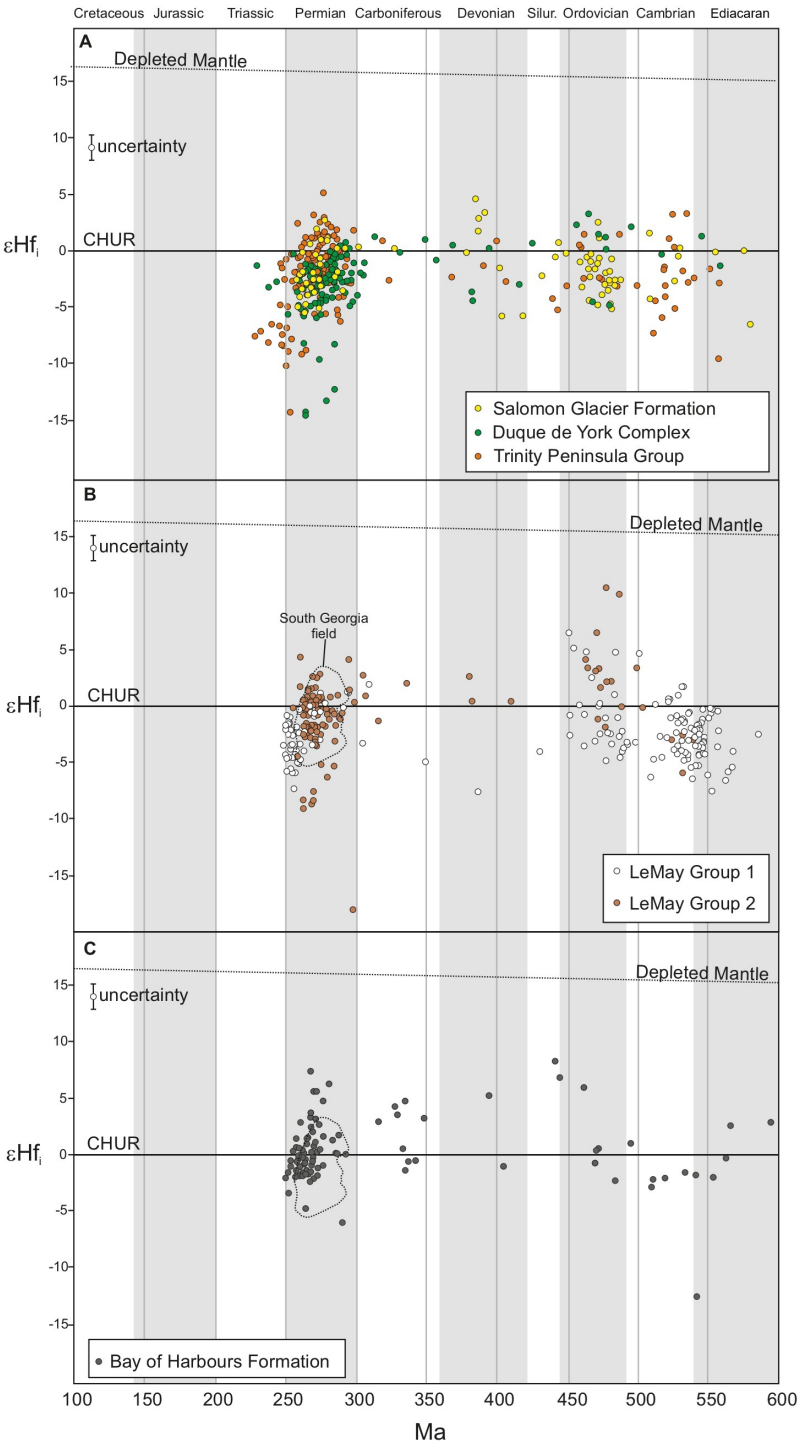

FIG. 7. U-Pb zircon ages ($^{238}U/^{206}Pb$) versus initial εHf values for zircon grains from late Permian metasedimentary successions examined as part of this study. Vertical grey and white bars represent geological periods. **A.** Drygalski Fjord Complex (South Georgia), Trinity Peninsula Group (Antarctic Peninsula), Duque de York Complex (Patagonia) (Barbeau *et al.*, 2010; Fanning *et al.*, 2011; Castillo *et al.*, 2016; this study). **B.** LeMay Group accretionary complex (Riley *et al.* 2023a). **C.** Bay of Harbours Formation (Riley *et al.*, 2025). Full Lu-Hf dataset is provided in Supplementary Table S2. Dashed lines in B and C encompass the late Permian South Georgia sample data shown in A. CHUR: Chondritic uniform reservoir.

Also plotted in figure 7 are Lu-Hf values from late Permian accretionary complex from Alexander Island (LeMay Group; Riley *et al.*, 2023b) (Fig. 7B) and the late Permian deltaic sandstones of the Bay of Harbours Formation from the Falkland/Malvinas Islands (Riley *et al.*, 2025) (Fig. 7C). The Bay of Harbours Formation is correlated with the upper Balfour Formation of the Karoo Basin, South Africa (Riley *et al.*, 2025) (Fig. 4) and can be considered a proxy for the late Permian Karoo Basin, for which no Lu-Hf data are available. The εHf_i range for the LeMay Group overlaps with that of the Salomon Glacier Formation, particularly LeMay Group 2. The range defined by the Bay of Harbours Formation (Fig. 7C) exhibits only limited overlap with the distribution of Salomon Glacier Formation data and generally lacks the more evolved values (<-3) of the Salomon Glacier Formation and the Trinity Peninsula Group/Duque de York Complex.

6. Discussion

Eagles and Eisermann (2020) examined plate kinematic reconstructions of the Scotia Sea and established that only half of South Georgia's proposed translation can be readily accounted for, assuming a 'starting' position in a back-arc setting adjacent to Tierra del Fuego. As a consequence, they challenged existing correlations to South America based on similarities in stratigraphy, tectonic setting and detrital zircon geochronology as being non-unique and equally explicable through geological links to southern Africa and East Antarctica. Their Early Jurassic reconstruction (Fig. 6B), which we use as an early Mesozoic proxy, places South Georgia adjacent to Coats Land and the Theron Mountains of East Antarctica, and adjacent to the Natal Embayment, with close links to southern Africa. Eagles and Eisermann (2020) suggested the presence of a newly recognised plate ('Skytrain'; Fig. 6B) that was hypothesised from sea floor architecture in the Falkland/Malvinas Basin. Their model also requires a South American setting for the Falkland/Malvinas Islands and negates the requirement for long distance translation of the South Georgia microcontinent.

In contrast, our analysis demonstrates strong evidence in favour of a connection between the late Permian accretionary successions of South Georgia with the mid-late Permian accretionary complexes of the northern Antarctic Peninsula and parts of Tierra del Fuego. We agree with Eagles and Eisermann (2020) that the application of detrital zircon geochronology for identifying exact provenance is often non-unique, particularly during periods of enhanced volcanism, deposition and sediment recycling. The late Permian is such an episode, with extensive silicic (zircon-rich) volcanism (*e.g.*, Choiyoi Province), widespread accretionary complexes (*e.g.*, Madre de Dios) and extensive sediment recycling and deposition in the hinterland (*e.g.*, Karoo Basin). However, our analysis of the U-Pb dataset from the late Permian metasedimentary units from South Georgia, supported by Lu-Hf isotopes, highlights several aspects in the data that argue against a direct connection to East Antarctica and South Africa, but strongly favour a close relationship to the northern Antarctic Peninsula and parts of Tierra del Fuego. The maximum depositional age of *ca*. 270 Ma of the Salomon Glacier Formation and other parts of the Drygalski Fjord Complex (Table 1), as well as the accretionary complexes of the Antarctic Peninsula and Patagonia, is also ubiquitous in East Antarctica, Karoo Basin and the southern Antarctic Peninsula (Riley *et al.*, 2025). However, a critical aspect of the age profile from the Salomon Glacier Formation and Drygalski Fjord Complex is the significant secondary age peak at *ca.* 470 Ma that is essentially absent from the hinterland successions in South Africa and East Antarctica, which are instead characterised by a secondary age peak at *ca*. 530 Ma, that is absent in South Georgia (Fig. 5). This Cambrian age peak may correlate with sources from granitoids associated with the Ross Orogen, or more likely represent recycling from early Palaeozoic sedimentary successions with more distal Gondwana sources. The *ca*. 470 Ma event is related to the widespread Famatinian magmatic arc and orogeny of South America (Rapela *et al.*, 2018; Otamendi *et al.*, 2020) that also extended via northeastern Patagonia (Pankhurst *et al.*, 2014) into eastern Graham Land of the northern Antarctic Peninsula (Riley *et al.*, 2012, 2023b). The age signature of the Ordovician Famatinian arc is evident in the recycled component of the late Permian metasedimentary rocks of Patagonia (Duque de York Complex, Cordillera Darwin) and the northern Antarctic Peninsula, and indicates relative proximity to a source region. Lu-Hf isotopes also support a close relationship between the Salomon Glacier Formation of South Georgia and the mid-Permian Trinity Peninsula Group of the Antarctic Peninsula, as well as components of the Duque de York Complex (Fig. 7).

Overall, the data support a close association between the South Georgia microcontinent and the northern Antarctic Peninsula, with a near-neighbour relationship in age profiles and Lu-Hf isotopes between the mid-late Permian accretionary complex of the Trinity Peninsula Group and the accretionary complex of the Salomon Glacier Formation. The Duque de York Complex is also likely to be relatively close, but we support a closer location to the Cordillera Darwin (Fig. 6A), particularly if a South Georgia location adjacent to the Isla de los Estados (Staten Island; Fig. 1) is favoured (Dalziel *et al.*, 2021). A detrital zircon age profile for a late Permian metasedimentary unit from the southern Cordillera Darwin (FO0642; Hervé *et al.*, 2010) is plotted in figures 4 and 5 and exhibits a prominent mid-late Permian age peak, and also a significant Early Ordovician age peak likely indicating derivation from the Famatinian arc or recycled unit.

Hervé *et al.* (2010) suggested that the Cordillera Darwin metamorphic complex has a distinct geological history from elsewhere in Patagonia and lies on the Scotia Plate and not the South American Plate. This scenario was supported by Riley *et al.* (2022) who developed a new dynamic plate model to demonstrate that the Cordillera Darwin metamorphic complex could have originated on the Antarctic Plate before translation to the Scotia Plate in the Eocene, along with the crustal blocks of the South Scotia Ridge (Fig. 1). Close paleo-location of the Cordillera Darwin, northern Antarctic Peninsula and the South Georgia microcontinent is supported by their overlap in the MDS plot (Fig. 4), although this only represents late Permian successions.

Placing South Georgia adjacent to the northern Antarctic Peninsula and Cordillera Darwin, particularly with a rotated Antarctic Peninsula, may negate the requirement for such lengthy lateral translation for the South Georgia microcontinent (Eagles and Eisermann, 2020), but still satisfies geological and tectonic correlations to the Staten Embayment (Dalziel *et al.*, 2021). Famatinian-age (*ca.* 470 Ma) zircons in South Georgia, Cordillera Darwin and the northern Antarctic Peninsula all suggest a nearby source. The εHf_i data (Fig. 7A) from the Salomon Glacier Formation for the Ordovician-age zircons (typically -5 to 0) are also consistent with the values reported by Rapela *et al.* (2018) from the Famatinian magmatic province. The Famatinian magmatic arc is generally considered to only extend as far south as the North Patagonian Massif (Pankhurst *et al.*, 2014; Rapela *et al.*, 2018), but with well-defined age peaks in the recycled sedimentary record of the northern Antarctic Peninsula (Riley *et al.*, 2023b), a more southerly extent is likely (Castillo *et al.*, 2020). Isolated outcrops of Early Ordovician magmatism in the north-eastern Antarctic Peninsula (Riley *et al.*, 2012) confirm this.

7. Conclusions

Using U-Pb and Lu-Hf detrital zircon analysis we demonstrate that the late Permian accretionary complex of South Georgia (Drygalski Fjord Complex) has a close association in depositional age and common source to metasedimentary units from the northern Antarctic Peninsula, and also the southern Cordillera Darwin and Duque de York Complex of southern Patagonia. The mid-late Permian is dominated by widespread accretionary complexes and recycled sedimentary successions across West Gondwana, which are all characterised by prominent late Permian age signals (*ca*. 260-270 Ma). The late Permian units from South Georgia, the northern Antarctic Peninsula and southern Patagonia are also characterised by a significant secondary age peak at *ca*. 470 Ma, correlating with the Early Ordovician Famatinian magmatic arc.

Although mid-late Permian units from South Africa, Falkland/Malvinas Islands and East Antarctica all have similar maximum depositional ages to the accretionary complexes of South Georgia, they lack a significant secondary age peak at *ca*. 470 Ma and are instead characterised by a mid-Cambrian age peak at *ca.* 530 Ma, typical of Cambrian recycled material of East Antarctica.

We favour a late Permian-early Mesozoic paleo-location of South Georgia adjacent to the northern Antarctic Peninsula and the Cordillera Darwin, all located on the Antarctic Plate, prior to closure of the Rocas Verdes Basin and subsequent translation of South Georgia and Cordillera Darwin to the Scotia Plate.

We rule out close links between South Georgia and South Africa/East Antarctica as proposed by Eagles and Eisermann (2020) in their Skytrain Plate model.

Acknowledgements

This study is part of the British Antarctic Survey Polar Science for a Sustainable Planet programme,

funded by the Natural Environmental Research Council. The original samples were collected by B. Storey and Ch. Bell and their detailed field observations were critical for our interpretations. M. Evans prepared samples for zircon separation, H. Jeon, A. Karlsson and K. Lindén provided support at the NordSIMS facility (supported by the Swedish Research Council infrastructure grant 2021-00276) and Ben Evans assisted with analyses at UCL. This paper has benefited from the helpful contributions of J. Bastías-Silva, D. Bertin, P. Castillo, J. Malone, B. Pankhurst and P. Stone. This is NordSIMS contribution number 809.

Data availability

The data that support this research are all available as supplementary files linked to this article. Full datasets are also hosted at the British Antarctic Survey's Polar Data Centre https://doi.org/10.5285/270714e6-f141-4c01-8a13-2bdfaca80ced

References

Barbeau, D.L.; Davis, J.T.; Murray, K.E.; Valencia, V.; Gehrels, G.E.; Zahid, K.M.; Gombosi, D.J. 2010. Detrital-zircon geochronology of the metasedimentary rocks of north-western Graham Land. Antarctic Science 22 (1): 65-78. https://doi.org/10.1017/S095410200999054X

Beaver, D.G.; Kent, D.V.; Dalziel, I.W.D. 2022. Paleomagantic constraints from South Georgia on the tectonic reconstruction of the Early Cretaceous Rocas Verdes marginal basin system of southernmost South America. Tectonics 41 (2): e2021TC006990. https://doi.org/10.1029/2021TC006990

Bouvier, A.; Vervoort, J.D.; Patchett, P.J. 2008. The Lu-Hf and Sm-Nd isotopic composition of CHUR: constraints from unequilibrated chondrites and implications for the bulk composition of terrestrial planets. Earth and Planetary Science Letters 273 (1-2): 48-57. https://doi.org/10.1016/j.epsl.2008.06.010

Carter, A.; Curtis, M.; Schwanethal, J. 2014. Cenozoic tectonic history of the South Georgia microcontinent and potential as a barrier to Pacific-Atlantic through flow. Geology 42 (4): 299-302. https://doi.org/10.1130/G35091.1

Castillo, P.; Fanning, C.M.; Hervé, F.; Lacassie, J.P. 2016. Characterization and tracing of Permian magmatism in the south-western segment of the Gondwanan margin; U-Pb age, Lu-Hf and O isotopic compositions of detrital zircons from metasedimentary complexes of northern Antarctic Peninsula and western Patagonia. Gondwana Research 36: 1-13. https://doi.org/10.1016/j.gr.2015.07.014

Castillo, P.; Fanning, C.M.; Riley, T.R. 2020. Zircon O and Hf isotope constraints on the genesis of Permian-Triassic magmatic and metamorphic rocks in the Antarctic Peninsula and correlations with Patagonia. Journal of South American Earth Sciences 104: 10 p. https://doi.org/10.1016/j.jsames.2020.102848

Clayton, R.A.S. 1982. A preliminary investigation of the Geochemistry of greywackes from South Georgia. British Antarctic Survey Bulletin 51: 89-109.

Craddock, J.P.; Fitzgerald, P.; Konstantinou, A.; Nereson, A.; Thomas, R.J. 2017. Detrital zircon provenance of upper Cambrian-Permian strata and tectonic evolution of the Ellsworth Mountains, West Antarctica. Gondwana Research 45: 191-207. https://doi.org/10.1016/j.gr.2016.11.011

Curtis, M.L. 2011. Geological Map of South Georgia (1:250 000 scale). *In* BAS GEOMAP2 Series, Sheet 4. British Antarctic Survey, Cambridge, UK.

Curtis, M.L.; Flowerdew, M.J.; Riley, T.R.; Whitehouse, M.J.; Daly, J.S. 2010. Andean sinistral transpression and kinematic partitioning in South Georgia. Journal of Structural Geology 32 (4): 464-477. https://doi.org/10.1016/j.jsg.2010.02.002

Dalziel, I.W.D.; Dott, R.H.; Winn, R.D.; Bruhn, R.L. 1975. Tectonic relations of South Georgia Island to the Southernmost Andes. Geological Society of America Bulletin 86 (7): 1034-1040. https://doi.org/10.1130/0016-7606(1975)86<1034:TROSGI>2.0.CO;2

Dalziel, I.W.D.; Macdonald, D.I.M.; Stone, P.; Storey, B.C. 2021. South Georgia microcontinent: Displaced fragment of the southernmost Andes. Earth Science Reviews 220: 103671. https://doi.org/10.1016/j.earscirev.2021.103671

Eagles, G. 2010. South Georgia and Gondwana's Pacific Margin: Lost in translation? Journal of South American Earth Sciences 30 (2): 65-70. https://doi.org/10.1016/j.jsames.2010.04.004

Eagles, G.; Eisermann, H. 2020. The Skytrain plate and tectonic evolution of southwest Gondwana since Jurassic times. Scientific Reports 10: 1-17. https://doi.org/10.1038/s41598-020-77070-6

Elliot, D.H.; Fanning, C.M.; Laudon, T.S. 2016. The Gondwana Plate margin in the Weddell Sea sector: Zircon geochronology of Upper Paleozoic (mainly Permian) strata from the Ellsworth Mountains and eastern Ellsworth Land, Antarctica. Gondwana Research 29 (1): 234-247. https://doi.org/10.1016/j.gr.2014.12.001

Fanning, C.M.; Hervé, F.; Pankhurst, R.J.; Rapela, C.W.; Kleiman, L.E.; Yaxley, G.M.; Castillo, P. 2011. Lu-Hf isotope evidence for the provenance of Permian detritus in accretionary complexes of western Patagonia and the northern Antarctic Peninsula region. Journal of South American Earth Sciences 32 (4): 485-496. https://doi.org/10.1016/j.jsames.2011.03.007

Flowerdew, M.J.; Daly, J.S.; Riley, T.R. 2007. New Rb-Sr mineral ages temporally link plume events with accretion at the margin of Gondwana. United States Geological Survey (USGS) Open-File Report 2007-1047, Short Research Paper 012: 4 p. https://doi.org/10.3133/ofr20071047SRP012

Flowerdew, M.J.; Tyrell, S.; Riley, T.R.; Whitehouse, M.J.; Mulvaney, R.W.; Leat, P.T.; Marschall, H.R. 2012. Distinguishing East and West Antarctic sediment sources using the Pb isotope composition of detrital K feldspar. Chemical Geology 292-293: 88-102. https://doi.org/10.1016/j.chemgeo.2011.11.006

Galbraith, R.; Laslett, G. 1993. Statistical models for mixed fission track ages. Nuclear Tracks and Radiation Measurements 21 (4): 459-470. https://doi.org/10.1016/1359-0189(93)90185-C

Hervé, F.; Fanning, C.M.; Pankhurst, R.J. 2003. Detrital zircon age patterns and provenance of the metamorphic complexes of southern Chile. Journal of South American Earth Sciences 16 (1): 107-123. https://doi.org/10.1016/S0895-9811(03)00022-1

Hervé, F.; Fanning, C.M.; Pankhurst, R.J.; Mpodozis, C.; Klepeis, K.; Calderón, M.; Thomson, S.N. 2010. Detrital zircon SHRIMP U-Pb age study of the Cordillera Darwin Metamorphic Complex of Tierra del Fuego: sedimentary sources and implications for the evolution of the Pacific margin of Gondwana. Journal of the Geological Society 167 (3): 555-568. https://doi.org/10.1144/0016-76492009-124

Jeon, H.; Whitehouse, M.J. 2015. A critical evaluation of U-Pb calibration schemes used in SIMS zircon geochronology. Geostandards and Geoanalytical Research 39 (4): 443-452. https://doi.org/10.1111/j.1751-908X.2014.00325.x

Livermore, R.; McAdoo, D.; Marks, K.M. 1994. Scotia Sea tectonics from high-resolution satellite gravity. Earth and Planetary Science Letters 123 (1-3): 255-268. https://doi.org/10.1016/0012-821X(94)90272-0

Macdonald, D.I.M. 1982. Palaeontology and ichnology of the Cumberland Bay Formation, South Georgia. British Antarctic Survey Bulletin 57: 1-14

Macdonald, D.I.M.; Storey, B.C.; Thomson, J.W. 1987. South Georgia, BAS GEOMAP Series, Sheet 1, 1:250,000, Geological Map and Supplementary Text. British Antarctic Survey: 63 p. Cambridge.

Mair, B.F. 1987. The Geology of South Georgia: VI. Larsen Harbour Formation. British Antarctic Survey Scientific Reports No. 111: 60 p.

Mukasa, S.B.; Dalziel, I.W.D., 1996. Southernmost Andes and South Georgia Island, North Scotia Ridge: zircon U-Pb and muscovite $^{40}Ar/^{39}Ar$ age constraints on tectonic evolution of Southwestern Gondwanaland. Journal of South American Earth Sciences 9 (5-6): 349-365. https://doi.org/10.1016/S0895-9811(96)00019-3

Otamendi, J.E.; Cristofolini, E.A.; Morosini, A.; Armas, P.; Tibaldi, A.M.; Camilletti, G.C. 2020. The geodynamic history of the Famatinian arc, Argentina: A record of exposed geology over the type section (latitudes 27°-33° south). Journal of South American Earth Sciences 100: 102558. https://doi.org/10.1016/j.jsames.2020.102558

Pankhurst, R.J.; Rapela, C.W.; López de Luchi, M.G.; Rapalini, A.E.; Fanning, C.M.; Galindo, C., 2014. The Gondwana connections of northern Patagonia. Journal of the Geological Society 171 (3): 313-328. https://doi.org/10.1144/jgs2013-081

Pettigrew, T.H. 1981. The geology of Annenkov Island. British Antarctic Survey Bulletin 53: 213-254. https://nora.nerc.ac.uk/id/eprint/524741

Rapela, C.W.; Pankhurst, R.J.; Casquet, C.; Dahlquist, J.A.; Fanning, C.M.; Baldo, E.G.; Galindo, C.; Alasino, P.H.; Ramacciotti, C.D.; Verdecchia, S.O.; Murra, J.A.; Basei, M.A.S. 2018. A review of the Famatinian Ordovician magmatism in southern South America: evidence of lithosphere reworking and continental subduction in the early proto-Andean margin of Gondwana. Earth-Science Reviews 187: 259-285. https://doi.org/10.1016/j.earscirev.2018.10.006

Riley, T.R.; Flowerdew, M.J.; Whitehouse, M.J. 2012. U-Pb ion-microprobe zircon geochronology from the basement inliers of eastern Graham Land, Antarctic Peninsula. Journal of the Geological Society 169 (4): 381-393. https://doi.org/10.1144/0016-76492011-142

Riley, T.R.; Carter, A.; Leat, P.T.; Burton-Johnson, A.; Bastías, J.; Spikings, R.A.; Tate, A.J.; Bristow, C.S. 2019. Geochronology and geochemistry of the northern Scotia Sea: a revised interpretation of the North and West Scotia ridge junction. Earth and Planetary Science Letters 518: 136-147. https://doi.org/10.1016/j.epsl.2019.04.031

Riley, T.R.; Carter, A.; Burton-Johnson, A.; Leat, P.T.; Hogan, K.A.; Bown, P.R. 2022. Crustal block origins of the South Scotia Ridge. Terra Nova 34 (6): 495-502. https://doi.org/10.1111/ter.12613

Riley, T.R.; Millar, I.L.; Carter, A.; Flowerdew, M.J.; Burton-Johnson, A.; Bastías, J.; Storey, C.D.; Castillo, P.; Chew, D.; Whitehouse, M.J. 2023a. Evolution of an accretionary complex LeMay Group and terrane translation in the Antarctic Peninsula. Tectonics 42 (2). https://doi.org/10.1029/2022TC007578

Riley, T.R.; Burton-Johnson, A.; Flowerdew, M.J.; Poblete, F.; Castillo, P.; Hervé, F.; Leat, P.T.; Millar, I.L.; Bastías, J.; Whitehouse, M.J. 2023b. Palaeozoic-Early Mesozoic geological history of the Antarctic Peninsula and correlations with Patagonia: Kinematic reconstructions of the proto-Pacific margin of Gondwana. Earth-Science Reviews 236: 104265. https://doi.org/10.1016/j.earscirev.2022.104265

Riley, T.R.; Carter, A.; Hunter, M.A.; Millar, I.L.; Flowerdew, M.J.; Curtis, M.L.; Hodgson, D.A. 2025. Provenance and correlation of Permian successions from the Falkland/Malvinas Islands with West Gondwana: implications for a Natal Embayment palaeo-location. Journal of the Geological Society 182 (4): https://doi.org/10.1144/jgs2024-282

Sláma, J.; Košler, J.; Condon, D.J.; Crowley, J.L.; Gerdes, A.; Hanchar, J.M.; Horstwood, M.S.A.; Morris, G.A.; Nasdala, L.; Norberg, N.; Schaltegger, U.; Schoene, B.; Tubrett, M.N.; Whitehouse, M.J. 2008. Plešovice zircon-a new natural reference material for U-Pb and Hf isotopic microanalysis. Chemical Geology 249 (1-2): 1-35. https://doi.org/10.1016/j.chemgeo.2007.11.005

Söderlund, U.; Patchett, P.J.; Vervoort, J.D.; Isachsen, C.E. 2004. The ^{176}Lu decay constant determined by Lu-Hf and U-Pb isotope systematics of Precambrian mafic intrusions: Earth and Planetary Science Letters 219 (3-4): 311-324. https://doi.org/10.1016/S0012-821X(04)00012-3

Stacey, J.S.; Kramers, J.D. 1975. Approximation of terrestrial lead evolution by a two-stage model. Earth and Planetary Science Letters 26 (2): 207-221. https://doi.org/10.1016/0012-821X(75)90088-6

Storey, B.C. 1983. The geology of South Georgia: V. Drygalski Fjord Complex. British Antarctic Survey Scientific Reports 107: 88 p.

Tanner, P.W.G.; Rex, D.C. 1979. Timing of events in an Early Cretaceous Island arc marginal basin system on South Georgia. Geological Magazine 116 (3): 167-179. https://doi.org/10.1017/S0016756800043582

Trouw, R.A.J.; Passchier, C.W.; Simoes, L.S.A.; Andreis, R.R.; Valeriano, C.M. 1997. Mesozoic tectonic evolution of the South Orkney Microcontinent, Scotia arc, Antarctica. Geological Magazine 134 (3): 383-401. https://doi.org/10.1017/S0016756897007036

Vermeesch, P. 2013. Multi-sample comparison of detrital age distributions. Chemical Geology 341: 140-146. https://doi.org/10.1016/j.chemgeo.2013.01.010

Vermeesch, P. 2018. IsoplotR: a free and open toolbox for geochronology. Geoscience Frontiers 9 (5): 1479-1493. https://doi.org/10.1016/j.gsf.2018.04.001

Vermeesch, P. 2021. Maximum depositional age estimation revisited. Geoscience Frontiers 12 (2): 843-850. https://doi.org/10.1016/j.gsf.2020.08.008

Viglietti, P.A.; Frei, D.; Rubidge, B.S.; Smith, R.M.H. 2018. U-Pb detrital zircon dates and provenance data from the Beaufort Group (Karoo Supergroup) reflect sedimentary recycling and air-fall tuff deposition in the Permo-Triassic Karoo foreland basin. Journal of African Earth Sciences 143: 59-66. https://doi.org/10.1016/j.jafrearsci.2017.11.006

Whitehouse, M.J.; Kamber, B.S. 2005. Assigning dates to thin gneissic veins in high-grade metamorphic terranes: A cautionary tale from Akilia, southwest Greenland. Journal of Petrology 46 (2): 291-318. https://doi.org/10.1093/petrology/egh075

Manuscript received: June 18, 2025; revised/accepted: November 06, 2025; available online: January 30, 2026.